Biosensors and Bioelectronics 135 (2019) 153–159

Contents lists available at ScienceDirect

Biosensors and Bioelectronics

journal homepage: www.elsevier.com/locate/bios

Facile one-step fabrication of glucose oxidase loaded polymeric nanoparticles decorating MWCNTs for constructing glucose biosensing platform: Structure matters

Sheng Xu[a,c], Yuheng Zhang[a], Ye Zhu[b], Jie Wu[a], Kaiyin Li[a], Geyu Lin[a], Xiaojie Li[a], Ren Liu[b], Xiaoya Liu[a,*], Ching-Ping Wong[c]

[a] Key Laboratory of Synthetic and Biological Colloids, Ministry of Education, School of Chemical and Material Engineering, Jiangnan University, 1800 Lihu Avenue, Wuxi, 214122, Jiangsu Province, PR China
[b] International Joint Research Center for Photoresponsive Molecules and Materials, Jiangnan University, 1800 Lihu Avenue, Wuxi, 214122, Jiangsu Province, PR China
[c] School of Materials Science and Engineering, Georgia Institute of Technology, 771 Ferst Drive NW, Atlanta, GA, 30332, United States

ARTICLE INFO

Keywords:
Enzymatic biosensor
Glucose oxidase
MWCNTs
Co-assembly
Enzyme immobilization
Glucose detection

ABSTRACT

A novel and robust enzymatic biosensing platform with high sensitivity is developed based on facile one-step assembled bio-nanocomposites with enzymes-loaded polymeric nanoparticles decorating multi-walled carbon nanotubes (MWCNTs). An amphiphilic copolymer PAVE containing photo-cross-linkable coumarin segments and carboxylic groups was co-assembled with MWCNTs in aqueous solution while encapsulating the model enzyme namely glucose oxidase (GOx) simultaneously, generating necklace-like bio-nanocomposites (GOx@PAVE-CNTs) with GOx-loading polymeric nanoparticles as nanobeads and MWCNTs as conducting micron-string. Then the GOx@PAVE-CNTs bio-nanocomposites were electro-deposited onto electrode surface and a robust biosensing complex film with porous network structure was formed after following photo-cross-linking. Consequently, an enzymatic glucose biosensor was successfully constructed. The biosensor exhibited ultrafast response (< 3 s) to glucose with a considerably wide linear range (1.0 μM ~ 5 mM) and a low detection limit (0.36 μM) for glucose detection. High sensitivity and selectivity of the biosensor toward glucose were also well demonstrated. Furthermore, the biosensor showed exceptionally good stability and reproducibility. More importantly, the glucose biosensor was practically used for glucose detection from human urine and serum samples with satisfactory results. As a proof-of-concept strategy, this facile and effective strategy for biosensor fabrication is of considerable interest because of its versatility to be generalized to many other enzymatic biosensor systems, exhibiting promising and practical potential in bio-medical and life health applications.

1. Introduction

Diabetes mellitus, a serious common metabolic disease caused by excess glucose accumulation in human blood, has become a worldwide headache due to the resulting overwhelming social and economic consequences (Wu et al., 2011; Locke et al., 2016). Though remarkable progress in modern medical science and technology has been achieved, it is rather costly and time-consuming to cure or prevent diabetes nowadays. In order to improve the treatment efficiency, quantitative detection and real-time monitoring of glucose levels are of significant importance and great necessity (Rines et al., 2016). In addition, it is also crucial to monitor glucose in fermentation of food industry because that glucose content directly influence the quality of food products (Verstrepen et al., 2004). Therefore, new strategies and sensing platforms for monitoring the accumulation level of glucose was and is always a hot topic in both scientific and industrial fields.

Among various reported strategies, enzymatic biosensor has long played a leading role since it was firstly proposed by Clark and Lyons in 1962 (Clark and Lyons, 1962; Reyes-De-Corcuera et al., 2018). Using enzymes for molecular recognition, enzymatic biosensors have been preferred over other chemical sensors thanks to its ultra-high specificity towards target analyte (Bollella and Gorton, 2018). For example, glucose oxidase (GOx) is the most widely used transducing enzyme in enzymatic glucose biosensors because of the specific catalytic activity towards glucose in biological system (Bankar et al., 2009). However, the problem related with enzymatic biosensor is that enzyme molecules are usually with large size and the redox centers are deeply buried with thick protein layers, resulting in poor electron shuttling across the

* Corresponding author.
E-mail address: lxy@jiangnan.edu.cn (X. Liu).

https://doi.org/10.1016/j.bios.2019.04.017
Received 1 February 2019; Received in revised form 26 March 2019; Accepted 9 April 2019
Available online 13 April 2019
0956-5663/ © 2019 Elsevier B.V. All rights reserved.

active reaction sites and electrode surface (Pakapongpan and Poo-arporn, 2017). In addition, enzymes on the sensor electrode surface tend to change the conformation and lose activities, leading to unsatisfactory long-term stability of the sensing performance (Lin et al., 2004). In order to improve the overall sensing performance of enzymatic biosensor for practical applications, the key lies in how to effectively integrate the biological enzymes onto the sensor electrode. Not only the amount, but also the activity of the immobilized biological enzyme must be ensured (Das et al., 2016). Various nanomaterials including polymers, noble metal nanoparticles, sol-gel matrices and nanocomposites have been widely used as supports to immobilize enzymes on sensor electrode surface (Zdarta et al., 2018). These nanomaterials can provide a larger specific surface area for loading more enzymes, a good microenvironment for protecting biological enzymes and an efficient electrical contact with the enzymes' active sites, leading to a significant improvement of the sensing performance of biosensors.

Recently, benefiting from the unique properties of carbon nanotubes (CNTs) including remarkably high aspect ratio, good biocompatibility, high electrical conductivity and electrocatalytic activity (Zhang et al., 2019; Schroeder et al., 2019), integration of CNTs with polymers for new polymer/CNTs nanocomposites with synergistic structural and functional properties has demonstrated great strengths in chemical sensors and biosensors (Gupta et al., 2018; Salavagione et al., 2014; Barsan et al., 2015). A lot of polymer/CNTs nanocomposites were synthesized and used as support materials for enzyme immobilizations, based on which numerous enzymatic biosensors have been generated (Valentini et al., 2013; Buber et al., 2017). However, most of these polymer/CNTs nanocomposites are casually prepared by simple complexion of polymer and CNTs, leading to bulky form of polymers on CNTs surfaces with relatively low enzyme immobilization efficiency. In addition, enzymes were directly immobilized onto the polymer/CNTs nanocomposites surface in most of these enzymatic biosensors. In this case, enzymes would easily deteriorate over short days, leading to unsatisfactory overall bio-sensing performance such as poor long-term sensing stability. Thus, to give full play to the synergetic advantages of both the polymer and CNTs for enzyme immobilizations, ingenious design and synthesis of polymer/CNTs nanocomposites as bio-sensing material is of significant importance for advancing enzymatic biosensor in real applications. Recently, our group has developed a new type of molecularly imprinted hybrid polymer/MWCNTs material by co-assembly of amphiphilic random copolymer with multi-walled carbon nanotubes (MWCNTs) while incorporating a small molecule namely paracetamol as template molecule simultaneously. The resultant molecularly imprinted sensors show excellent performance towards paracetamol as the hybrids combined both the advantages of polymer nanoparticles and the long conducting MWCNTs (Xu et al., 2018). Inspired by the highly effective molecularly imprinting strategy of small molecules, it is highly envisioned that if enzymes could be effectively attached to CNTs with the help of amphiphilic copolymers which could interact with both enzymes and CNTs. If feasible, a novel enzyme-loading polymer/CNTs nanocomposite with high loading capacity and high conductivity would be generated, based on which a versatile enzymatic biosensor platform will be established with significant importance in practice.

In the present study, we developed a versatile and robust enzymatic biosensing platform via the one-step co-assembly of MWCNTs with an amphiphilic copolymer poly(acrylic acid-r-(7-(4-vinylbenzyloxy)-4-methyl coumarin)-r-ethylhexyl acrylate) (PAVE) while incorporating biological enzyme as the molecular recognition element simultaneously. As a proof of concept, glucose oxidase (GOx) was chosen as a representative enzyme aiming at constructing a highly effective biosensor for specific glucose determination. Driven by certain interactions, a long-conducting necklace-like nanocomposites with enzyme-loading polymeric nanoparticles decorating MWCNTs (denoted as GOx@PAVE-CNTs NCs) was prepared in aqueous solution. For biosensor fabrication, the nanocomposites were then deposited on

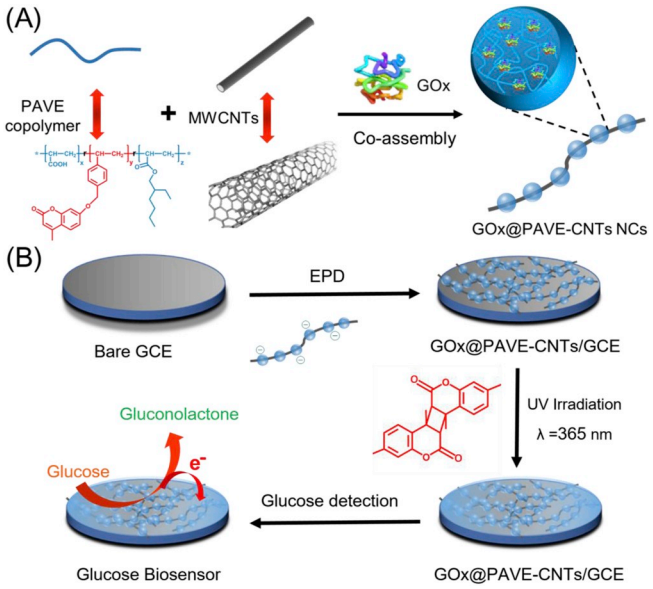

Scheme 1. Schematic illustration of the enzymatic glucose biosensor fabrication. (A) Preparation of the long conducting enzyme-loading hybrid nanocomposite GOx@PAVE-CNTs via one-step co-assembly. (B) Preparation process of glucose biosensor via direct electrophoretic deposition (EPD) of GOx@PAVE-CNTs onto glassy carbon electrode (GCE) surface and subsequent photo-cross-linking.

electrode surface via direct electrophoretic deposition, forming a robust networked complex sensing coating after subsequent photo-cross-linking. The whole fabrication strategy of GOx@PAVE-CNTs NCs and enzymatic glucose biosensor was shown in Scheme 1. The photo-cross-linking of these polymeric PAVE nanoparticles would endow high GOx loading capacity with inhibited enzyme leakage in the bio-nanocomposites. Meanwhile, the long conducting MWCNTs through the nanocomposites would provide numerous "electronic paths" for electrons shuttling between GOx and electrode transducer. As a consequence, the prepared enzymatic biosensor exhibited fast electrochemical response and high sensitivity toward glucose. The nanocomposite was characterized and the sensing performance of the purposed biosensor was also investigated, and the results are shown below. This versatile sensing platform is expected to be generalized to many other enzymatic biosensor devices for practical point-of-care biomedical applications.

2. Experimental

All experimental details are provided in Supporting Information.

3. Results and discussion

3.1. Preparation and characterization of GOx@ PAVE-MWCNTs NCs

Thanks to the presence of aromatic rings containing VMc segments in PAVE polymer chains, PAVE copolymers and long conductive MWCNTs can be non-covalently bonded together through "π-π" stacking interactions (Tan et al., 2018). By employing MWCNTs as long conductive fillers and GOx as specific recognition receptor in the polymer assembly process, it is highly expected to generate a novel bio-nanocomposite (GOx@PAVE-CNTs) with integrated functionalities. The preparation of the enzyme loading bio-nanocomposite GOx@PAVE-CNTs was schematically shown in Scheme 1A. During the co-assembly process of PAVE copolymers and MWCNTs, GOx would be incorporated into the polymeric nanobeads along MWCNTs simultaneously by hydrogen-bonding interaction and hydrophobic interaction, giving birth

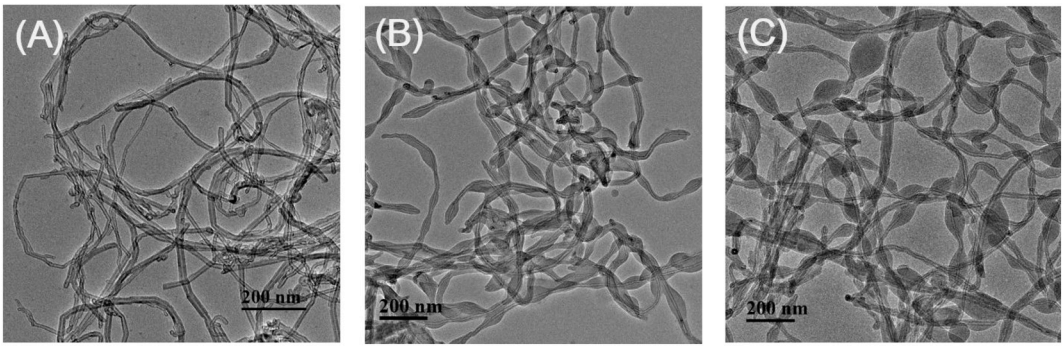

Fig. 1. TEM images of (a) pristine MWCNTs, (b) PAVE-CNTs nanocomposites and (c) GOx@PAVE-CNTs bio-nanocomposites.

to unified GOx@PAVE-CNTs nanocomposite.

The morphologies of GOx@PAVE-CNTs and the control samples of pristine MWCNTs, PAVE-CNTs were characterized by TEM. Fig. 1A shows that pristine MWCNTs with pipe diameter of 20 nm mutually entangle together on account of strong intertubes van der Waals interaction. Interestingly, for PAVE-CNTs, the amphiphilic copolymer assembled onto MWCNTs surfaces, forming "necklace-like" structured morphology with PAVE polymeric NPs decorating along MWCNTs string (Fig. 1B). Similar morphologies have also been reported with co-assembly of amphiphilic copolymers and CNTs (Kang and Taton, 2003; Shin et al., 2005). According to TEM results and previous literatures, the formation of this interesting hierarchical structure can be fundamentally explained as follows. Benefiting from π-conjugated VMc segments in the polymer backbone, PAVE copolymers first anchored onto MWCNTs surface driven by the strong π-π stacking interactions. Since water is a poor solvent to hydrophobic moieties (VMc and EHA) in PAVE copolymers, the incorporation of water would lead to gradual formation of polymer aggregates along MWCNTs from swollen random polymer coils, resulting in long "necklace-like" PAVE-CNTs nanohybrids. During the co-assembly process of PAVE and MWCNTs, many GOx enzyme molecules were brought into PAVE-CNTs nanocomposites driven by hydrogen bonding interactions between the PAVE copolymer and GOx molecules as well as hydrophobic interactions from the amphiphilic nature of polymer, thus generating enzymes-loading GOx@PAVE-CNTs bio-nanocomposites. As shown in Fig. 1C, after the incorporation of GOx, the obtained GOx@PAVE-CNTs biocomposites still exhibit "necklace-like" morphology. However, obvious increase in size of the polymer beads along MWCNTs surface can be observed, indicating the successful incorporation of GOx enzymes into the PAVE-CNTs nanocomposites. The nanometer size of PAVE NPs can provide high specific surface area for improving the GOx immobilization capability, while the long conducting MWCNTs strings can greatly enhancing the charge transfer behavior among the whole biosensing interfaces. Therefore, the "necklace-like" GOx@PAVE-CNTs would show high potential for application in biosensor systems. In addition, the presence of solvophilic PAVE nanobeads on MWCNTs surface endows this GOx-loading bio-nanocomposites with good long-term dispersibility in aqueous solution through steric and electrostatic repulsion. Fig. S4 shows the digital photographs of different MWCNTs containing dispersions in water. Unmodified MWCNTs show obvious settlement in water because of its hydrophobic surface. In contrast, with the help of amphiphilic PAVE copolymer on MWCNTs surfaces, both PAVE-CNTs dispersion and GOx@PAVE-CNTs dispersion still exhibited homogenous state without visualized sedimentation even after one month storage.

FT-IR Spectrascopy, UV–visible absorption spectroscopy (UV-vis) and X-ray photoelectron spectroscopy (XPS) were applied to further confirm the co-assembly of GOx enzymes into PAVE-CNTs during the assembly process. As shown in Fig. S5, The presence of two characteristic amide I and II peaks of GOx (Baghayeri et al., 2014) in the FT-IR spectrum of GOx@PAVE-CNTs well evidence the successful presence of the GOx molecules in the unified bio-nanocomposite. UV–vis spectroscopy is a useful conformational probe for monitoring the possible conformational changes of biological proteins (Li et al., 2013). The UV–vis spectra of pure GOx solution, dispersions of PAVE colloidal NPs (control sample), GOx@PAVE NPs and GOx@PAVE-CNTs NCs were performed. As shown in Fig. 2A, native GOx showed three absorption peaks at 278 nm (characteristic peak of polypeptide chains), 383 and 456 nm (oxidized form of flavin groups in protein) (Liu and Hu, 2007). An obvious absorption peak at 320 nm appeared in the spectrum of PAVE NPs, which is derived from the characteristic of coumarin groups in the polymer skeleton (Jiang et al., 2007). For both spectra of GOx@PAVE NPs and GOx@PAVE-CNTs NCs, peaks which just coincide with those of native GOx enzyme can be observed besides the peak from PAVE copolymer, indicating the successful incorporation of GOx enzymes in GOx@PAVE-CNTs NCs with well preservation of native enzyme structure. XPS is also a powerful tool to investigate the chemical composition of materials, which has been effectively demonstrated in protein immobilization or adsorption (Artyushkova and Atanassov, 2013). XPS survey spectra of pure GOx, PAVE NPs, GOx@PAVE NPs, and GOx@PAVE-CNTs NCs were measured and displayed in Fig. 2B. As shown, the XPS spectrum of PAVE NPs shows only two peaks at 282 eV for C 1s and 529 eV for O 1s. However, for both GOx@PAVE NPs and GOx@PAVE-CNTs, another peak at 397 eV can be observed, which is

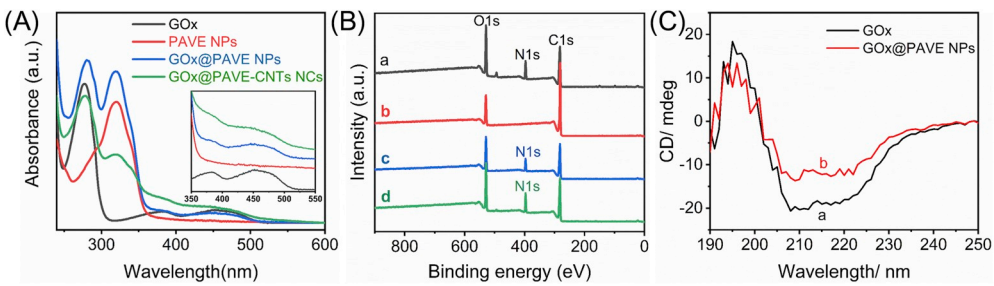

Fig. 2. (A) UV-Vis and (B) XPS survey spectra of (a) pure GOx, (b)PAVE NPs, (c)GOx@PAVE NPs and (d) GOx@PAVE-CNTs NCs. (C) CD spectra of (a) pure GOx and (b) GOx@PAVE NPs.

consistent with the N 1s peak from pure GOx enzymes (amide bonds in polypeptide chains). These XPS results provide powerful evidence that GOx molecules were successfully co-assembled into the GOx@PAVE-CNTs NCs.

For enzymatic biosensors, the sensing materials used for enzyme immobilization should provide a favorable microenvironment to preserve the bioactivity of enzymes. Driven by some noncovalent interactions between GOx and PAVE copolymer, GOx molecules were encapsulated to the polymeric NPs along MWCNTs surfaces during the co-assembly process. To illustrate the compatibility of PAVE copolymer to GOx, circular dichroism (CD) spectra of native GOx and GOx@PAVE NPs were measured. In general, CD spectrum between 190 nm and 250 nm corresponds to n→π* electronic transition of peptide. The spectrum recorded in this far-UV region will change sensitively if the secondary structure and conformation enzyme conformation changes (Wu et al., 2010). As shown in Fig. 2C, GOx@PAVE-CNTs shows similar CD spectrum compared to that of native GOx, indicating that the immobilized GOx molecules well maintain their conformation as original enzyme states in PAVE-CNTs nanocomposites. The slight decrease in peak intensities is due to intermolecular interactions between GOx and PAVE copolymers, which can retard GOx leaking from the PAVE-CNTs nanocomposites (Ren et al., 2009). The CD results illustrate that the PAVE copolymer matrix could afford GOx molecules with a favorable biological microenvironment, verifying that GOx would retain its biological activity in the GOx@PAVE-CNTs bio-nanocomposite.

3.2. Fabrication and characterization of the enzymatic biosensor

The whole fabrication process of the enzymatic biosensor is illustrated in Scheme 1B. Thanks to the effective immobilization of GOx into PAVE-CNTs, the resultant GOx@PAVE-CNTs nanocomposites were applied as biosensing material to constructe a novel enzymatic biosensor. Due to large amount of carboxyl groups on PAVE polymers, the GOx@PAVE-CNTs nanocomposites are negatively charged in aqueous solution. For biosensor fabrication, the GOx@PAVE-CNTs dispersion were deposited on to the surface of glassy carbon electrode (GCE) conducted by direct electrophoretic deposition (EPD). The schematic diagram of the EPD cell for GOx@PAVE-CNTs deposition is shown in Fig. 3A. The EPD equipment is quite simple and the whole electrophoretic deposition process is easy to operate, cost-effective and environmentally friendly. Most importantly, compared traditional "drop-casting" method for electrode modification, EPD may greatly avoid individual variation between electrodes with the same modified sensing materials (Ata et al., 2018; Zhang et al., 2018). After that, the GOx@PAVE-CNTs deposited GCE was placed under UV light for photo-cross-linking, obtaining complex biosensing film modified electrode as GOx@PAVE-CNTs/GCE.

The morphology of the composite biosensing film on sensor surface was observed by SEM (Fig. 3B). As shown, a mass of hierarchically structured GOx@PAVE-CNTs bio-nanocomposites gather together, developing fibrous and interlaced network sensing film. Notably, thanks to the photo-dimerization property of coumarin moieties without the need of extra photo-initiator (Jiang et al., 2007), polymer chains among the composite film would cross-link to form integral network structure under UV irradiation. As a result, these cross-linked polymers around GOx molecules would provide reliable microenvironment for retaining the biological activity of GOx as well as preventing GOx leakage from the electrode surface. In addition, MWCNTs throughout the composite sensing film would act as "electronic tunnels" to accelerate electron shuttling across the biological recognition sites and electrode transducer. Moreover, thanks to MWCNT locating in the axis of the GOx@PAVE-CNTs, MWCNTs would also behave like "signal collectors" to fast transmit the response signals from recognition reaction. Thanks to the stable structural integrity and high effective enzyme loading capacity of the biosensing GOx@PAVE-CNTs film, high biological recognition response and high sensing stability of the biosensor are expected when being applied in detection environment.

Electrochemical impedance spectroscopy (EIS) was applied for further probing the interfacial natures of different surface coated electrodes. In principle, electron transfer and diffusion behaviors can be inferred from a typical Nyquist plot of an EIS spectrum. The diameter of the depressed semicircular part corresponds to charge transfer resistance (R_{ct}) of the sensing materials on the electrode surface. Therefore, by means of the reversible reaction of redox probe like [Fe

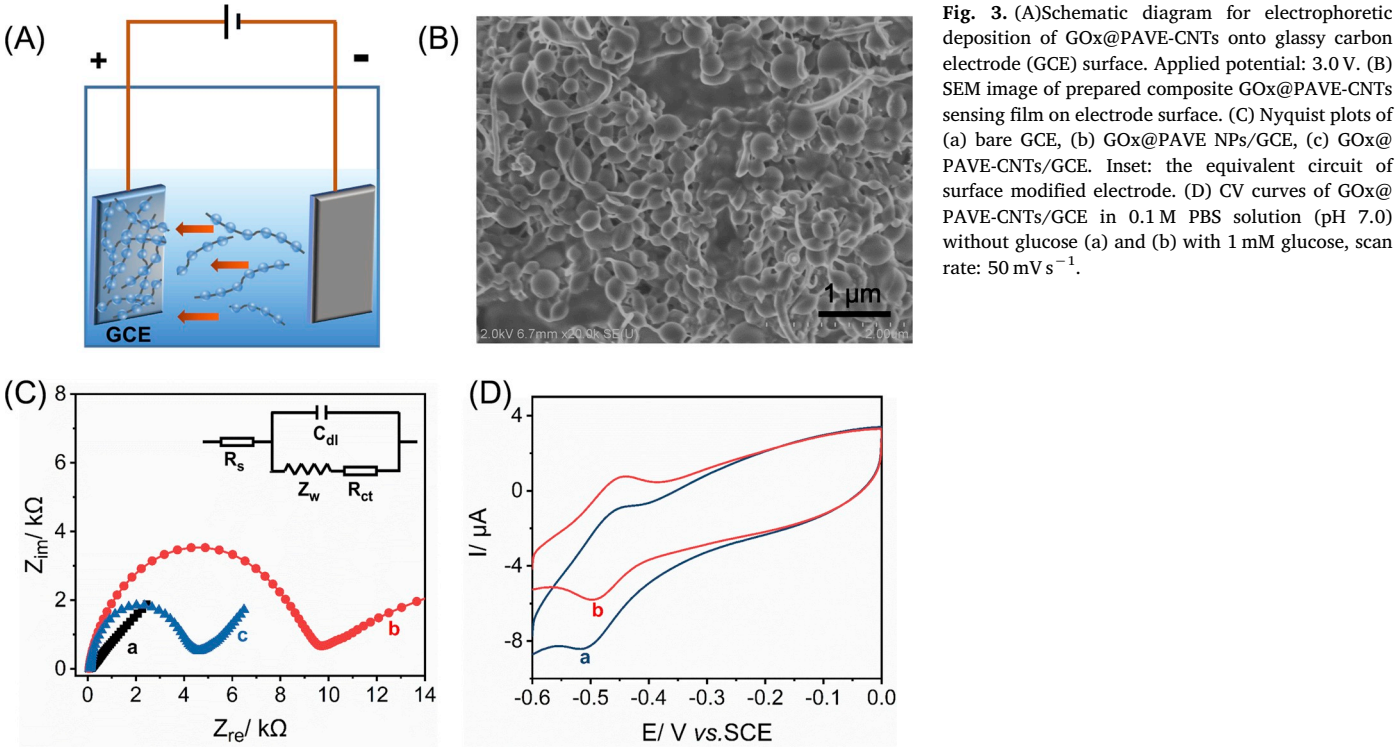

Fig. 3. (A)Schematic diagram for electrophoretic deposition of GOx@PAVE-CNTs onto glassy carbon electrode (GCE) surface. Applied potential: 3.0 V. (B) SEM image of prepared composite GOx@PAVE-CNTs sensing film on electrode surface. (C) Nyquist plots of (a) bare GCE, (b) GOx@PAVE NPs/GCE, (c) GOx@PAVE-CNTs/GCE. Inset: the equivalent circuit of surface modified electrode. (D) CV curves of GOx@PAVE-CNTs/GCE in 0.1 M PBS solution (pH 7.0) without glucose (a) and (b) with 1 mM glucose, scan rate: 50 mV s^{-1}.

$(CN)_6]^{3-}$/$[Fe(CN)_6]^{4-}$, the interfacial properties of the sensing film would be monitored at electrode interface (Randviir and Banks., 2013). To fully illuminate the role of MWCNTs, GOx-loaded polymeric nanoparticles GOx@PAVE NPs without MWCNTs were prepared and used as control samples for GOx@PAVE-CNTs bio-nanocomposites. The corresponding EIS plots are shown in Fig. 3C, and the specific R_{ct} values were obtained by simulation according to the inset equivalent circuit. For bare GCE, the Nyquist plot is like a straight line, indicating almost unimpeded electron transfer on electrode surface. The R_{ct} value of bare GCE is quite small of about 77 Ω. However, a significantly larger R_{ct} value around 8368 Ω was obtained for GOx@PAVE NPs modified electrode, which is ascribed to that an insulating film from these non-conductive GOx@PAVE NPs hinder electron transfer across the electrode interface to a great extent. In contrast, after incorporation of MWCNTs, R_{ct} value of GOx@PAVE-CNTs/GCE (4039 Ω) decreases dramatically than that of GOx@PAVE NPs/GCE. The EIS results reveal that MWCNTs in the GOx@PAVE-CNTs bio-nanocomposites substantially enhance the electrical conductivity across sensor surface, demonstrating remarkable advantages of the "necklace-like" structured GOx@PAVE-CNTs nanocomposites as sensing materials in enzymatic biosensors. To illustrate the bioelectrocatalytic activity of the enzymatic biosensor, cyclic voltammetry (CV) was conducted using GOx@PAVE-CNTs/GCE in the absence (a) and presence of 1 mM (b) of glucose. As shown in Fig. 3D, well-defined redox peaks are observed in the absence of glucose (plot a). After addition of glucose solution into the blank PBS solution, the anodic peak current increased whereas the cathodic peak current decreased (plot b). The changes of redox peaks can be ascribed to the decrease in O_2 reduction current due to the depletion of O_2 in a biosensor by the mediated enzymatic process (Wooten et al., 2014). The CV results verify that the GOx well maintain its biocatalytic activity on the electrode surface (Baghayeri et al., 2017) and the fabricated GOx@PAVE-CNTs based biosensor can be potentially applied as an effective enzymatic biosensor for glucose sensing.

3.3. Analytical performance of enzymatic biosensor

3.3.1. Calibration curve

To illustrate our based strategy as highly effective enzymatic biosensing platform, the GOx@PAVE-CNTs bio-nanocomposites based biosensor was applied in glucose sensing. The sensing mechanism is shown in Supporting Information and the applied potential for glucose detection was optimized (Fig. S6). The sensing performance towards glucose was investigated by recording the amperometric response to successive glucose addition with a sampling time of 30 s at an optimized working potential of 0.5 V. As shown in Fig. 4A, upon each addition of glucose at regular intervals, a rapid and stair-step increase in current response is observed. Excitingly, the glucose biosensor showed ultrafast response to glucose with a short response time within 3.0 s. Fig. 4B shows the calibration curve corresponding to varying current responses and glucose concentrations. As shown, the current response and glucose concentration exhibits significantly good linear relationship in two sections. The first section spans from 0.001 mM to 1 mM with a linear regression equation being presented as I (μA) = 0.0268 + 2.1971$C_{glucose}$ (mM) (R^2 = 0.999). The second linear regression equation can be expressed as I(μA) = 0.8106 + 1.4834Cglucose (mM) (R^2 = 0.998) in the concentration range from 1 mM to 5 mM. The detection limit (LOD), calculating according to previous method (Xu et al., 2017), is as low as 0.36 μM (S/N = 3). To make a comparison, sensing performances of the GOx@PAVE-CNTs based biosensor and those of previous enzymatic glucose biosensors based on GOx-CNTs composites were listed in Table S1. As shown, the GOx@PAVE-CNTs based enzymatic biosensor shows much wider linear range than other glucose biosensors. Furthermore, the LOD of our biosensor towards glucose determination reaches a very low concentration, which can be applied in trace glucose monitoring in biomedical diagnostics and human health fields. Notably, the response time of our glucose biosensor is as short as less than 3 s. Therefore, our biosensor shows almost fastest response among these glucose biosensors. The exceptional sensing performance can be attributed to the synergistic strengths from the PAVE nanobeads and the micron long conducting MWCNTs throughout the GOx@PAVE-CNTs bio-nanocomposites. For one thing, PAVE NPs along MWCNTs provide much larger specific surface area than many traditional composite sensing material with bulky forms, thus improving the enzyme immobilization capability and providing extremely abundant recognition sites. For another, the MWCNTs throughout the interpenetrating GOx@PAVE-CNTs based networked composite film can serve as long conducting "electronic tunnels", which indirectly shorten the distance from the active sites of enzymes to electrode surface and greatly accelerate electron shuttling across the sensing interface. As a result, the "necklace-like" GOx@PAVE-CNTs bio-nanocomposite based enzymatic biosensor demonstrated outstanding sensing performance towards glucose detection with exceptionally high sensitivity and ultrafast response.

3.3.2. Anti-interference study

For an enzymatic biosensor, the most outstanding merit is its recognition specificity to target analyte with providing discrimination of other interferents in complex system (Wu et al., 2018). To demonstrate the anti-interference ability of our GOx@PAVE-CNTs based glucose biosensor, interferents including uric acid (UA), ascorbic acid (Vitamin C, VC), dopamine (DA) and L-lysine (L-lys) were used as typical representatives due to the inevitable coexistence with glucose in real samples (such as human serum) (Pakapongpan and Poo-arporn, 2017). The anti-interference ability was assessed by recording the amperometric response by sequentially and alternately adding 0.5 mM glucose, and the interferents with the same concentration of UA, VC, DA, and L-lys. As shown in Fig. 5A, compared with glucose induced current response, the presence of these interferents shows negligible current response (detailed explanation is shown in Supporting Information).

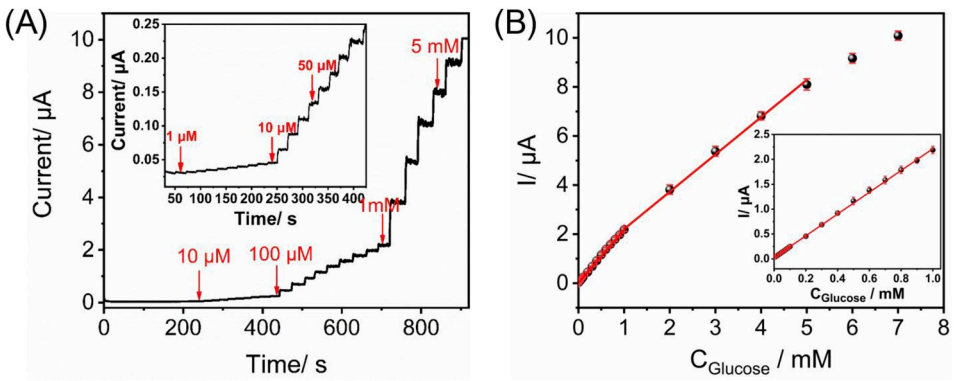

Fig. 4. (A) Amperometric response of the GOx@PAVE-CNTs based biosensor to successively injecting glucose to 0.1 M PBS solution (pH 7.0) at working potential of 0.5 V (vs. SCE); glucose concentration increases from 1 μM to 7 mM. Inset: enlarged view of amperometric response curve in lower glucose concentration range. (B) Calibration curve of the response current versus glucose concentrations. Inset: enlarged view of calibration curve in lower concentration range between 1 μM and 1 mM.

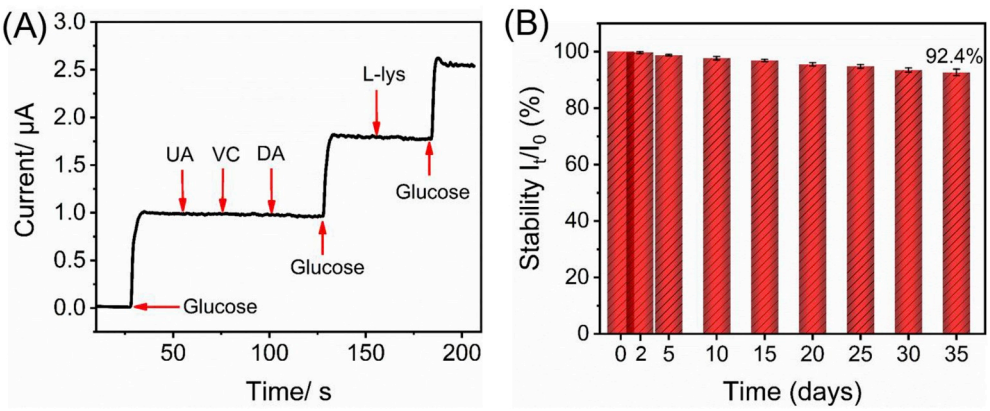

Fig. 5. (A) Interference test of the glucose biosensor with successive addition of 0.5 mM glucose, 0.5 mM of each interfering species including uric acid (UA), ascorbic acid (Vitamin C, VC), Dopamine (DA) and L-lysine (L-lys), respectively in 0.1 M PBS (pH 7.0); (B) The histogram of long-term stability measurement of the enzymatic glucose biosensor based on GOx@PAVE-CNTs for 35 days, where I_0 and I_t are the initial current and the response current after t days, respectively.

Therefore, the GOx@PAVE-CNTs based enzymatic biosensor has excellent anti-interference ability which would be a promising candidate for specific glucose determination in real complex aqueous samples.

3.3.3. Reproducibility, repeatability and stability

Reproducibility is an extremely important characteristic for successful electrochemical biosensors. To investigate the reproducibility of the glucose biosensor, five independent glucose biosensors are fabricated following the same preparation procedure with GOx@PAVE-CNTs nanocomposites as biosensing materials. The current response of each electrode was recorded in the same glucose solution (0.1 M PBS) with glucose concentration of 0.5 mM, which exhibited almost similar response for all the five glucose biosensors. A low relative standard deviation (RSD = 3.27%) of the five biosensors current response demonstrated the credible reproducibility of the developed enzymatic glucose biosensor. The repeatability (or repetitivity) of the biosensor was studied by consecutively recording the current responses corresponding to 0.5 mM glucose solution for eight times (Fig. S7). An acceptable relative standard deviation (RSD) of 3.55% for these eight repetitive measurements were obtained, demonstrating the good repeatability of the developed glucose biosensor.

The long-term stability of enzymatic biosensors is a challenging issue due to the instability of immobilized enzymes. For the stability test, the peak currents of the same glucose biosensor were recorded toward the same glucose concentration over 35 days with the biosensor being stored in 0.01 M PBS (pH 7.4) at 4 °C. As shown in Fig. 5B, even after 35 days, the current response to initial value still retain at 92.4%, verifying that the GOx@PAVE-CNTs based biosensor has excellent long-term stability. The excellent sensing stability is definitely ascribed to enhanced structure stability of the photo-cross-linked GOx@PAVE-CNTs bio-nanocomposites. To illustrate the effectiveness of photo-cross-linking on the sensor performance, the influence of UV irradiation on the sensor performance was investigated, which indicates that photo-cross-linking did not damage enzymes but enhanced the sensing performance (Fig. S8). In addition, the current responses of biosensors based GOx@PAVE-CNTs bio-nanocomposites with and without photo-cross-linking at the storage of 30 days were compared. As shown in Fig. S9, compared to crosslinked GOx@PAVE-CNTs based biosensor with high retention of response current, un-crosslinked biosensor dramatically deteriorates its current response which may be attributed to GOx molecules debonding from swollen PAVE NPs along MWCNTs surfaces. The photo-cross-linking of PAVE nanobeads generates robust polymer network, which would not only provide compatible microenvironment for preserving the enzyme activity but also effectively suppress enzyme leakage from the electrode surface when applying in the aqueous environment (Chang et al., 2003). The stability results indicate that the GOx@PAVE-CNTs based glucose biosensor is stable and reliable to be potentially used for glucose determination.

3.3.4. Practical performance in real samples

To investigate feasible application of the GOx@PAVE-CNTs based enzymatic glucose biosensor in real samples, the sensing performance was studied in both the human urine samples from healthy young man and human serum samples from local hospital. For glucose determination, the original samples were diluted with 0.1 M PBS and the glucose detection were conducted using a spike recovery method (Márquez et al., 2017; Zhao et al., 2018). The results of glucose detection from human urine and human serum samples are summarized in Table S2. For original human urine samples, no glucose was detected from all the three samples. The recoveries of spiked samples of human urine varied from 94.6% to 104.8% with highly acceptable RSD values between 2.43% and 3.21%. For original human serum samples, glucose concentrations were detected by our glucose biosensor and calculated according to the calibration equation, which are within the healthy range of blood glucose in human body. The recoveries of spiked samples of human serum are between 95.8% and 98.2% with desirable RSD values. All the recovery data and the respective RSD values are in acceptable range for application in real samples. These highly satisfactory results from real samples well illustrated that the GOx@PAVE-CNTs biosensor would serve as a practical and effective sensing platform for monitoring glucose contents in biomedical diagnose and health monitoring.

4. Conclusions

In summary, we presented a novel and robust enzymatic biosensing platform with high sensitivity and fast response based on facile one-step co-assembly of oxidative enzymes with amphiphilic poly(AA-co-VMc-co-EHA) (PAVE) copolymer and MWCNTs. The glucose oxidase (GOx) as a model enzyme was simultaneously encapsulated during the co-assembly process of the photo-cross-linkable PAVE copolymer with MWCNTs in aqueous solution. The obtained enzyme-loaded nanocomposite (GOx@PAVE-CNTs) showed necklace-like structure with GOx-containing polymeric nanoparticles as the nanobeads and MWCNTs as the long string through these nanobeads. For biosensor fabrication, the GOx@PAVE-CNTs nanocomposite as a whole was deposited onto electrode surface by a facile electrophoretic deposition technique. After subsequent photo-cross-linking, GOx@PAVE-CNTs formed interlaced porous composite sensing film on the electrode surface, and thus an enzymatic glucose biosensor was successfully constructed. The biosensor exhibited ultrafast response (less than 3 s) to glucose determination with significantly wide linear response range (1.0 μM ~ 5 mM) and low detection limit (0.36 μM) for glucose detection. Thanks to the hierarchical structure of GOx@PAVE-CNTs which involves the synergistic effect of nanosized polymeric particles and the micron-long conducting MWCNTs, the biosensor showed high sensitivity and selectivity toward glucose. In addition, high sensing stability and reproducibility of the enzymatic biosensor were also demonstrated benefiting from the structural stability of the composite biosensing film

and the compatible microenvironment for enzymes preservation provided by photo-cross-linking of the amphiphilic copolymers. To our satisfaction, reliable results were obtained from both human urine and serum samples for glucose detection using the developed GOx@PAVE-CNTs based glucose biosensor, demonstrating a promising feature for practical application in biomedical diagnostics and human health monitoring. By virtue of the purposeful design of polymer structure, ongoing work in our lab will involve some functional monomers with high electro-activity and affinity to enzymes into the polymer framework, which is expected to bring out the most potential of polymer/CNTs nanocomposites as highly efficient biosensing material via one step co-assembly strategy. Overall, the present methodology demonstrates a facile, efficient and robust strategy for enzymatic biosensor fabrication, which can be generalized to many other enzymatic biosensor systems due to the versatility of polymer functionalization. The whole strategy will definitely provide useful reference and inspiration for new generation of biosensing devices and integrated sensing electronics.

Declaration of interests

The authors declare that they have no known competing financial interests or personal relationships that could have appeared to influence the work reported in this paper.

CRediT authorship contribution statement

Sheng Xu: Conceptualization, Methodology, Formal analysis, Investigation, Writing - original draft, Data curation, Visualization. **Yuheng Zhang:** Investigation, Data curation, Visualization. **Ye Zhu:** Methodology, Data curation, Validation. **Jie Wu:** Investigation, Visualization. **Kaiyin Li:** Investigation, Visualization. **Geyu Lin:** Investigation. **Xiaojie Li:** Writing - review & editing, Validation, Project administration, Funding acquisition. **Ren Liu:** Conceptualization, Validation, Supervision, Project administration, Funding acquisition. **Xiaoya Liu:** Conceptualization, Methodology, Formal analysis, Writing - review & editing, Validation, Project administration, Supervision, Funding acquisition. **Ching-Ping Wong:** Writing - review & editing, Supervision.

Acknowledgments

This work was supported by the National Natural Science Foundation of China (NSFC 21334001, 51573073, 51803079), the Postgraduate Research & Practice Innovation Program of Jiangsu Province (KYCX17_1428), and MOE & SAFEA for the 111 Project (B13025). Sheng Xu is thankful for the scholarship from Jiangnan University to pursue his study in Georgia Institute of Technology.

Appendix A. Supplementary data

Supplementary data to this article can be found online at https://doi.org/10.1016/j.bios.2019.04.017.

References

Artyushkova, K., Atanassov, P.X., 2013. ChemPhysChem 14, 2071–2080.
Ata, M.S., Poon, R., Syed, A.M., Milne, J., Zhitomirsky, I., 2018. Carbon 130, 584–598.
Baghayeri, M., Veisi, H., Veisi, H., Maleki, B., Karimi-Maleh, H., 2014. RSC Adv. 4, 49595–49604.
Baghayeri, M., Veisi, H., Ghanei-Motlagh, M., 2017. Sensor. Actuator. B Chem. 249, 321–330.
Bankar, S.B., Bule, M.V., Singhal, R.S., Ananthanarayan, L., 2009. Biotechnol. Adv. 27, 489–501.
Barsan, M.M., Ghica, M.E., Brett, C.M.A., 2015. Anal. Chim. Acta 881, 1–23.
Bollella, P., Gorton, L., 2018. Curr. Opin. Electrochem. 10, 157–173.
Buber, E., Kesik, M., Soylemez, S., Toppare, L., 2017. J. Electroanal. Chem. 799, 370–376.
Chang, K.S., Hsu, W.L., Chen, H.Y., Chang, C.K., Chen, C.Y., 2003. Anal. Chim. Acta 481, 199–208.
Clark, L.C., Lyons, C., 1962. Ann. N. Y. Acad. Sci. 102, 29–45.
Das, P., Das, M., Chinnadayyala, S.R., Singha, I.M., Goswami, P., 2016. Biosens. Bioelectron. 79, 386–397.
Gupta, S., Murthy, C.N., Prabha, C.R., 2018. Int. J. Biol. Macromol. 108, 687–703.
Jiang, J.Q., Qi, B., Lepage, M., Zhao, Y., 2007. Macromolecules 40, 790–792.
Kang, Y., Taton, T.A., 2003. J. Am. Chem. Soc. 125, 5650–5651.
Li, J., Yang, Z.J., Tang, Y., Zhang, Y.C., Hu, X.Y., 2013. Biosens. Bioelectron. 41, 698–703.
Lin, Y., Lu, F., Tu, Y., Ren, Z., 2004. Nano Lett. 4, 191–195.
Liu, H.Y., Hu, N.F., 2007. Electroanalysis 19, 884–892.
Locke, A.K., Cummins, B.M., Cote, G.L., 2016. ACS Sens. 1, 584–590.
Márquez, A., Jimenez-Jorquera, C., Dominguez, C., Muñoz-Berbel, X., 2017. Biosens. Bioelectron. 97, 136–142.
Pakapongpan, S., Poo-arporn, R.P., 2017. Mater. Sci. Eng. C 76, 398–405.
Randviir, E.P., Banks, C.E., 2013. Anal. Methods 5, 1098–1115.
Ren, X.L., Chen, D., Meng, X.W., Tang, F.Q., Du, A.M., Zhang, L., 2009. Colloids Surf., B 72, 188–192.
Reyes-De-Corcuera, J.I., Olstad, H.E., García-Torres, R., 2018. Annu. Rev. Food Sci. Technol. 9, 293–322.
Rines, A.K., Sharabi, K., Tavares, C.D.J., Puigserver, P., 2016. Nat. Rev. Drug Discov. 15, 786–804.
Salavagione, H.J., Díez-Pascual, A.M., Lázaro, E., Vera, S., Gómez-Fatou, M.A., 2014. J. Mater. Chem. 2, 14289–14328.
Schroeder, V., Savagatrup, S., He, M., Lin, S., Swager, T.M., 2019. Chem. Rev. 119, 599–663.
Shin, H.I., Min, B.G., Jeong, W., Park, C., 2005. Macromol. Rapid Commun. 26, 1451–1457.
Tan, K., Ma, Q., Luo, J., Xu, S., Zhu, Y., Wei, W., Liu, X.Y., Gu, Y., 2018. Biosens. Bioelectron. 117, 713–719.
Valentini, F., Fernandez, L.G., Tamburri, E., Palleschi, G., 2013. Biosens. Bioelectron. 43, 75–78.
Verstrepen, K.J., Iserentant, D., Malcorps, P., Derdelinckx, G., Van Dijck, P., Winderickx, J., Pretorius, I.S., Thevelein, J.M., Delvaux, F.R., 2004. Trends Biotechnol. 22, 531–537.
Wooten, M., Karra, S., Zhang, M., Gorski, W., 2014. Anal. Chem. 86, 752–757.
Wu, H.Y., Lee, C.J., Wang, H.F., Hu, Y., Young, M.G., Han, Y., Xu, F.J., Cong, H.B., Cheng, G., 2018. Chem. Sci. 9, 2540–2546.
Wu, P., Shao, Q., Hu, Y., Jin, J., Yin, Y., Zhang, H., Cai, C., 2010. Electrochim. Acta 55, 8606–8614.
Wu, Q., Wang, L., Yu, H., Wang, J., Chen, Z., 2011. Chem. Rev. 111, 7855–7875.
Xu, S., Lin, G.Y., Zhao, W., Wu, Q., Luo, J., Wei, W., Liu, X.Y., Zhu, Y., 2018. ACS Appl. Mater. Interfaces 10, 24850–24859.
Xu, S., Zhang, R.L., Zhao, W., Zhu, Y., Wei, W., Liu, X.Y., Luo, J., 2017. Biosens. Bioelectron. 92, 570–576.
Zdarta, J., Meyer, A.S., Jesionowski, T., Pinelo, M., 2018. Adv. Colloid Interface Sci. 258, 1–20.
Zhang, R., Ying, C., Gao, H., Liu, Q., Fu, X., Hu, S., 2019. Compos. Sci. Technol. 171, 218–225.
Zhang, R.L., Zhu, Y., Huang, J., Xu, S., Luo, J., Liu, X.Y., 2018. ACS Appl. Mater. Interfaces 10, 5926–5932.
Zhao, W., Zhang, R.L., Xu, S., Cai, J., Zhu, X.J., Zhu, Y., Wei, W., Liu, X.Y., Luo, J., 2018. Biosens. Bioelectron. 100, 497–503.